Applied Geography 155 (2023) 102952

Contents lists available at ScienceDirect

Applied Geography

journal homepage: www.elsevier.com/locate/apgeog

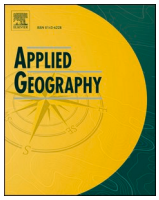

Bat bio-assisted sampling (BAS) for monitoring urban heat island

Alexandra Chudnovsky [a,2,*], Aya Goldshtein [b,1,2], Limor Shashua-Bar [c], Yossi Yovel [b,d,f,3], Oded Potchter [a,e,3]

[a] Porter School of Environment and Earth Sciences, Raymond & Beverly Sackler Faculty of Exact Sciences, Tel Aviv University, Israel
[b] School of Zoology, The George S. Wise Faculty of Life Sciences, Tel Aviv University, Israel
[c] Porter School of Environment and Earth Sciences, Department of Environmental Studies, Raymond & Beverly Sackler Faculty of Exact Sciences, Tel Aviv University, Israel
[d] Sagol School of Neuroscience, Tel Aviv University, Israel
[e] Department of Geography, Beit Berl College, Israel
[f] The Steinhardt Museum of Natural History, National Research Center for Biodiversity Studies, Tel-Aviv University, Israel

ARTICLE INFO

Handling Editor: J Peng

Keywords:
Urban heat island (UHI)
Air temperature
Biologically-assisted sampling (BAS)
Bats
Greenness
Greenness cooling effect

ABSTRACT

In this study, we demonstrate how urban-dwelling bats can be used to reconstruct Urban Heat Islands (UHI). We term this approach biologically-assisted sampling (BAS). We used Egyptian fruit bats to map the spatial air temperature (Tair) profile. To demonstrate the feasibility of using biologically-assisted sampled data set, we run mixed effects and Geographically Weighted Regression (GWR) models to estimate the impact of urban environment on Tair distribution. Our results suggest that vegetation is a very important mitigating factor in Tair. In the winter, we found an average Tair difference of 2–5 °C between densely urban and nearby vegetative/open areas. A distinct UHI spot was identified in the winter, centered on the Ayalon highway. These differences were lower during the summer night, probably due to a pronounced cooling sea breeze effect along the coastline. Our preliminary results also indicate that BAS sampling provide a 3D view of the UHI phenomenon: the change in Tair above the dense urban area was smaller than above the vegetative area. Since the differences in Tair between densely urban and open/green areas are the largest during the night hours, bats can serve as efficient agents to monitor UHI effects, despite the method limitations.

1. Introduction

The urban heat island (UHIs) phenomenon is characterized by much warmer metropolitan area than the non-urban spaces surrounding it (Oke, 1987). UHI with different magnitudes occur worldwide and are quite common in urban climates. UHI's affect citizens' comfort and have been found to be correlated to air pollution, heat stress and health (Saaroni et al., 2000; Ulpiani, 2021; Wang et al., 2021), and even intensified heat-related mortality (Brauer & Hystad, 2014; Luber & McGeehin, 2008; Zanobetti & Schwartz, 2008; Carreras et al., 2015; Smargiassi et al., 2009; Hankey and Marshall, 2017; Salvador et al., 2023).

Tair refers to the commonly measured air temperature in an aspirated shield at a height of 2 m above the ground in meteorological stations (WMO, 2018). Due to the nature of Tair measurements in urban meteorological stations, which are limited in number, their data are not spatially continuous, limiting analyses of spatial variability. Many studies have been conducted worldwide, and in the Tel Aviv area in particulate, to monitor the variability of Tair in the urban domain. For Tel-Aviv, these include: (1) conventional in-situ measurements combined with thermal sensors and satellite imagery (Deilami et al., 2018; Mandelmilch et al., 2020; Kim & Brown, 2021); (2) diurnal thermal variability analyses of different urban surfaces (Chudnovsky et al., 2004); (3) modeling the correlation between Tair and satellite-based surface temperature (Lensky & Dayan, 2015; Pelta & Chudnovsky, 2017; Pelta et al., 2016; Zhou et al., 2020); (4) estimating the thermal

* Corresponding author.
E-mail addresses: achudnov@tauex.tau.ac.il (A. Chudnovsky), goldaya@gmail.com (A. Goldshtein), sblimor@gmail.com (L. Shashua-Bar), yossiyovel@gmail.com (Y. Yovel), potchter@tauex.tau.ac.il (O. Potchter).
[1] Present address: Department of Collective Behavior, Max Planck Institute of Animal Behavior, Konstanz 78464, Germany.
[2] First authors contributed equally.
[3] Last authors contributed equally.

https://doi.org/10.1016/j.apgeog.2023.102952
Received 3 February 2023; Received in revised form 20 March 2023; Accepted 27 March 2023
Available online 16 April 2023

effect of different neighborhoods and locations across the city, including land covers, on temperature (Chudnovsky et al., 2004; Rotem-Mindali et al., 2015; Saaroni et al., 2000). However, accurate monitoring of Tair fields in the city domain at high temporal and spatial resolution remains a challenge. More Tair sampling locations are needed in locations that currently are restricted by meteorological or environmental limitations (only 3–7 sites in Gush Dan area provide temporal data). An important additional data source for environmental monitoring is the incorporation of mobile monitors and lightweight sensors on unmanned aerial vehicles (UAVs) or any other lightweight moving platform (Burgués & Marco, 2020; Kezoudi et al., 2021; Kuantama et al., 2019; Lugassi et al., 2022; Walendziuk et al., 2018). However, this technology is still limited due to regulatory restrictions, which differ for each country, ranging from permission to fly above urban areas to limited flight heights which, in many cases, is restricted to high altitudes rather than rooftop urban conditions (75–150 m) (Lugassi et al., 2022).

Bio-assisted sampling (BAS) includes the use of organisms to monitor the environment (i.e., physical and/or chemical), as well as, ecological processes and biodiversity via mounted low-footprint sensors (Greif & Yovel, 2019). These organisms can be plants (e.g., Carreras et al., 2005, 2009; Carreras & Pignata, 2002), humans, fish, insects, diatoms and others (Holt & Miller, 2010), and they can be used to estimate a human population's exposure to different environmental stressors in the air, water, food, soil, etc. (Hays et al., 2007; Lavi et al., 2016; Pollack et al., 2017; Santonen et al., 2015). The last decade has witnessed considerable advances in biologging, with the development of devices that allow tracking small animals for long periods with low-footprint sensors that provide information on their internal state and external surroundings (Wilmers et al., 2015). Tracking the environmental characteristics experienced by the animal (e.g., ambient temperature, humidity, pollution, etc.) provides new insight into its external state and enables a better understanding of the animals' behavior and the choices they make (Wilmers et al., 2015). Furthermore, monitoring the natural environment of animals that occupy niches that are difficult to access, using the animals themselves as data-collecting agents, may yield new insights into their habitats and their change with time. For example, recording the ambient temperature on-board elephant seals allowed mapping the temperature profile of the Western Antarctic Peninsula (Costa et al., 2010), and measuring the ambient temperature on-board king penguins provided information about the circulation patterns of water in the upper layers of the Southern Ocean (Charrassin et al., 2002).

1.1. Study goals

In this study, for the first time to the best of our knowledge, we evaluated the use of a BAS tool for UHI analyses. We attached miniature sensors to Egyptian fruit bats (*Rousettus aegyptiacus*) to monitor the spatial profile of Tair across the greater Tel Aviv area. Our aim was to generate a better temporal and spatial understanding of the impact of different neighborhoods with different urban morphologies on UHI development, serving as a complementary Tair to the existing stationary network. Two field experiments, performed in the winter and summer, were conducted in the greater Tel Aviv area in the evening-early morning hours (20:00 - and 02:30). Tair differences between urban areas and their rural surroundings are usually largest at night, making bats, with their nocturnal habit, ideal BAS agents to monitor the effects of UHIs.

2. Materials and methods

2.1. Study area

We selected the Tel Aviv metropolitan area, known as Gush Dan, for our study. Gush Dan, which includes Tel Aviv and adjacent cities, is the largest and most populated metropolitan area in Israel. It is located on the eastern shoreline of the Mediterranean Sea and is characterized by a Mediterranean climate. The climate in Tel Aviv is defined as Csa according to the Köppen classification (Köppen, 1931; Potchter & Saaroni, 1998). The climatic conditions are characterized by two main seasons: a hot, humid summer (mean temperature 23–30 °C, mean relative humidity 72–83%) and a mild, wet winter with stable weather episodes (average temperature 8–23 °C, average relative humidity 55–60%). The wind regime during the summer is influenced by the Mediterranean Sea breeze, which blows during the day from the west and northwest, and at nighttime from the east and southeast. In winter, the wind regime depends on the synoptic conditions and is therefore difficult to characterize (Bitan & Rubin, 1994). The city of Tel Aviv develops a mild UHI with maximum Tair differences on winter nights of up to 5 °C (Saaroni et al., 2000) and on summer nights and midday of up to 4 °C (Mandelmilch et al., 2020). Previous studies in the Tel Aviv metropolitan area have reported that urban vegetation can reduce Tair by up to 4 °C, depending on vegetation type and amount of canopy coverage (Cohen et al., 2012; Shashua-Bar et al., 2010; Shashua-Bar & Hoffman, 2000).

2.2. Data processing, analyses and field experiments: the methodological approach

Our study consisted of several steps as shown in Fig. 1. First, we examined the stability and accuracy of the lightweight Vesper air temperature sensor (Alexander Schwartz Developments (A.S.D) Inc., Haifa, Israel) by comparing its measurements with two well-calibrated ground-monitoring measurements for 24 h (step 1; experiment 1, Fig. 1): Tair measured at the nearest meteorological site and Tair measured by a Lufft XC200 sensor (Lufft, Stuttgart, Germany). The Lufft and Vesper sensors were placed next to each other and in the immediate vicinity of the ground-based Tair site. The Vesper system consists of a low-footprint docking station, a GPS sensor unit that also includes a temperature and relative humidity sensor (SHT31), and a 3.7 V LiPO battery. Vesper sensors have been previously used on bats to track their GPS locations (Egert-Berg et al., 2018; Goldshtein et al., 2021) and on UAVs to track temperature and humidity during a large field campaign (Lugassi et al., 2022).

In step 2, two BAS field experiments were conducted during winter and summer (experiments 2 and 3, Fig. 1). We used Egyptian fruit bats equipped with Vesper sensors to record their location and ambient temperature and mapped spatial Tair distribution across different land uses. These bats are central-place (colony) foragers (Daniel et al., 2008; Olsson & Brown, 2006) that forage up to tens of kilometers from their roost (cave) and return to their cave at the end of the night.

In parallel to the BAS campaign, (experiments 2 and 3, Fig. 1), a large field experiment was conducted in the Tel Aviv metropolis and served as validation (step 3; experiment 4, Fig. 1). These measurements provided extended meteorological information. In step 4, we studied the impact of different land uses on Tair variability by estimating the total vegetation cover and the fraction percentage of building surfaces within a 30 m × 30 m grid cell. We also visually inspected all locations where Tair was measured by the Vesper sensors that was mounted on the bats using high resolution (less than 1 m) air photo imagery (within ArcGIS software).

2.3. Using bats for BAS

The experiment was performed with capture permits from Israel National and Park Authority and was approved by the IACUC committee (permit Number L-12-031). The winter experiment was conducted on 10–11 January 2019 and the summer experiment on 20–21 June 2019 (20:00–02:30 a.m.).

During the winter experiment, 10 Egyptian fruit bats were caught using hand nets in their cave in Herzliya, a city that is ~10 km to the north of Tel Aviv and is considered part of the Tel Aviv metropolis, a few hours before sunset. A lightweight and miniature Vesper sensor (4.35 g in weight including battery and 16 × 34 × 3.5 mm in size) was mounted on the back of the bat using surgical cement (Fig. 1, upper left) and fall-

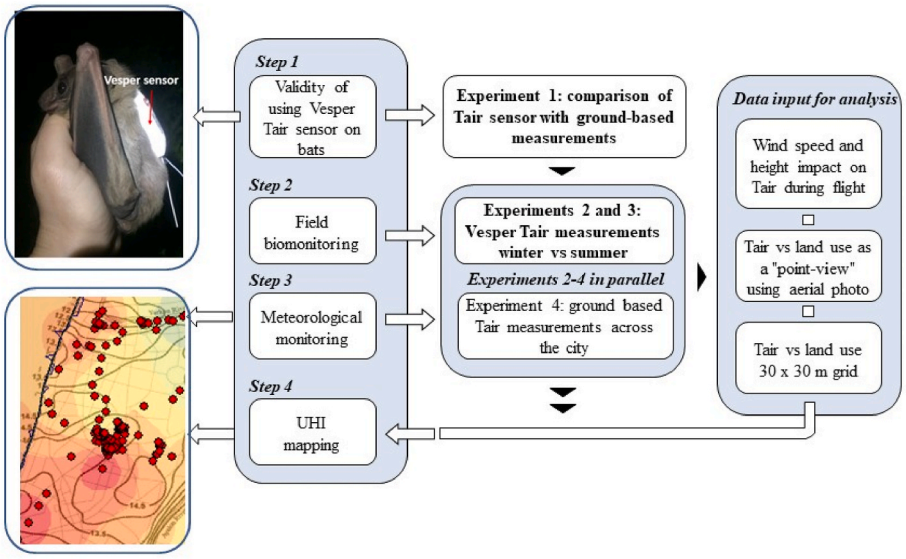

Fig. 1. General concept flow chart.

off a few days later (Cvikel et al., 2015; Egert-Berg et al., 2018; Goldshtein et al., 2021; Harten et al., 2020).

The Vesper is a multi-sensor, with a built-in GPS sensor, to which temperature and relative humidity (SHT31) sensor module was added. A telemetry unit was attached to the data logger (Holohil Systems Ltd., Carp, Ontario, Canada) to enable locating the GPS device when it fell off the bat. The total weight of the tracking device accounted for 6.9 ± 0.9% of the bat's body mass (158.1 ± 12.5 (g), n = 20), a weight that has been shown feasible for a bat to carry while commuting and foraging (Egert-Berg et al., 2018; Harten et al., 2020; Tsoar et al., 2011).

The bats were then translocated to Tel Aviv city center and released in five locations (two bats at each location during the winter). As expected, the bats flew back to their cave in Herzliya (Fig. 2). Five data loggers were successfully retrieved and used for the statistical analysis. Upon translocation (i.e., capture in their cave and release at a distant location), these bats usually commute back to a previously visited food tree or directly to their cave (Harten et al., 2020; Tsoar et al., 2011). We used these long commute flights to measure the UHIs of Tel Aviv at different altitudes above the ground (0–30 m) and compared the data to control measurements performed on the ground. We released the bats in such locations that on their commute back, they would fly above different landscapes—dense urban areas, parks and highways—thus enabling an assessment of the impact of the landscape on ambient temperature. We used the five bats from which the data loggers were recovered to monitor the UHIs around the city of Tel Aviv (Fig. 2A). Releasing the bats at the city center provided a measurement of Tair in a highly populated and densely built-up urban area, and a comparison with the largest green area in Tel Aviv (Yarkon Park, which the bats cross when flying back to their cave) (Fig. 2A). In addition, because these bats often use highways as landmarks when navigating (Harten et al., 2020), we were able to examine the influence of road constructions on the above-ground environmental temperature. The devices of only two bats were retrieved in the summer experiment.

2.4. Instrumentation: experiment 1

As we previously stated, different temperature sensors along with the Vesper sensor were tested simultaneously in the laboratory and outdoor conditions (Lugassi et al. 2022). Here we aimed to investigate how data obtained from Vesper differ from very stable and well-established sensors. The largest difference was during the midday hours (3.5 °C on the day of the experiment), when the temperature was at its maximum. Moreover, at midday, the sensor was exposed to the sun's radiation, which creates a bias in the temperature reading. The evening and night hours showed the closest agreement among all sensors. Therefore, the best time to conduct the field experiment was determined to be in the evening and through the night, matching the bats' biological clock and the time at which the UHI is at its peak.

2.5. Experimental set-up and data pre-processing testing bats behavior to get likely reliable Tair measurements: experiments 2–4

BAS of the environmental temperature was based on the bats' behavior. Every GPS point included information on the bat's location (latitude and longitude) and the altitude above the ellipsoid of the earth. The bats' altitude above ground was calculated by subtracting the height of the geoid and elevation above ground from the altitude above the ellipsoid. The geoid height was estimated using the EGM2008 Geopotential Model (with an accuracy of 0.001 m and the elevation above ground was estimated using SRTM3 (at a resolution of ~90 m). Previous estimates showed that this method results in altitude errors of approximately 10 m on average (Cvikel et al., 2014). Temperature data were assigned to the closest GPS point.

The bats' flight was divided into commute and foraging according to the straightness index, i.e., the ratio between the flight beeline and the path lengths of short flight segments (Benhamou, 2004). This index was calculated for each GPS point for segments of 2 min before and after the relevant point. Based on past experience (Harten et al., 2020), GPS points with a straightness index >0.5 were considered to represent commuting behavior, whereas points with lower values were considered to represent foraging behavior. However, in cases where the altitude above the surface was greater than 20 m and the speed was greater than 2 m/s, we assumed that the bat was not foraging, regardless of the straightness index. A threshold value for the bats speed was 8.3 ± 0.95 m/s (n = 4 bats). Moreover, by translocating the animals to a particular direction relative to their colony, one can achieve some control over their trajectory. Feeding the bats, for example, prior to their release will likely induce them take a more direct path home.

Importantly, to avoid temperature artifacts during foraging (e.g., influence of canopy temperature or perching near other bats), we excluded the foraging data from the analysis. The temperature response time for the sensors attached to the bats was set to 30 s based on our previous laboratory studies (Harten et al., 2020; Lugassi et al. 2022).

2.5.1. Meteorological monitoring at ground level as validation against BAS

The meteorological field survey was conducted during the winter on

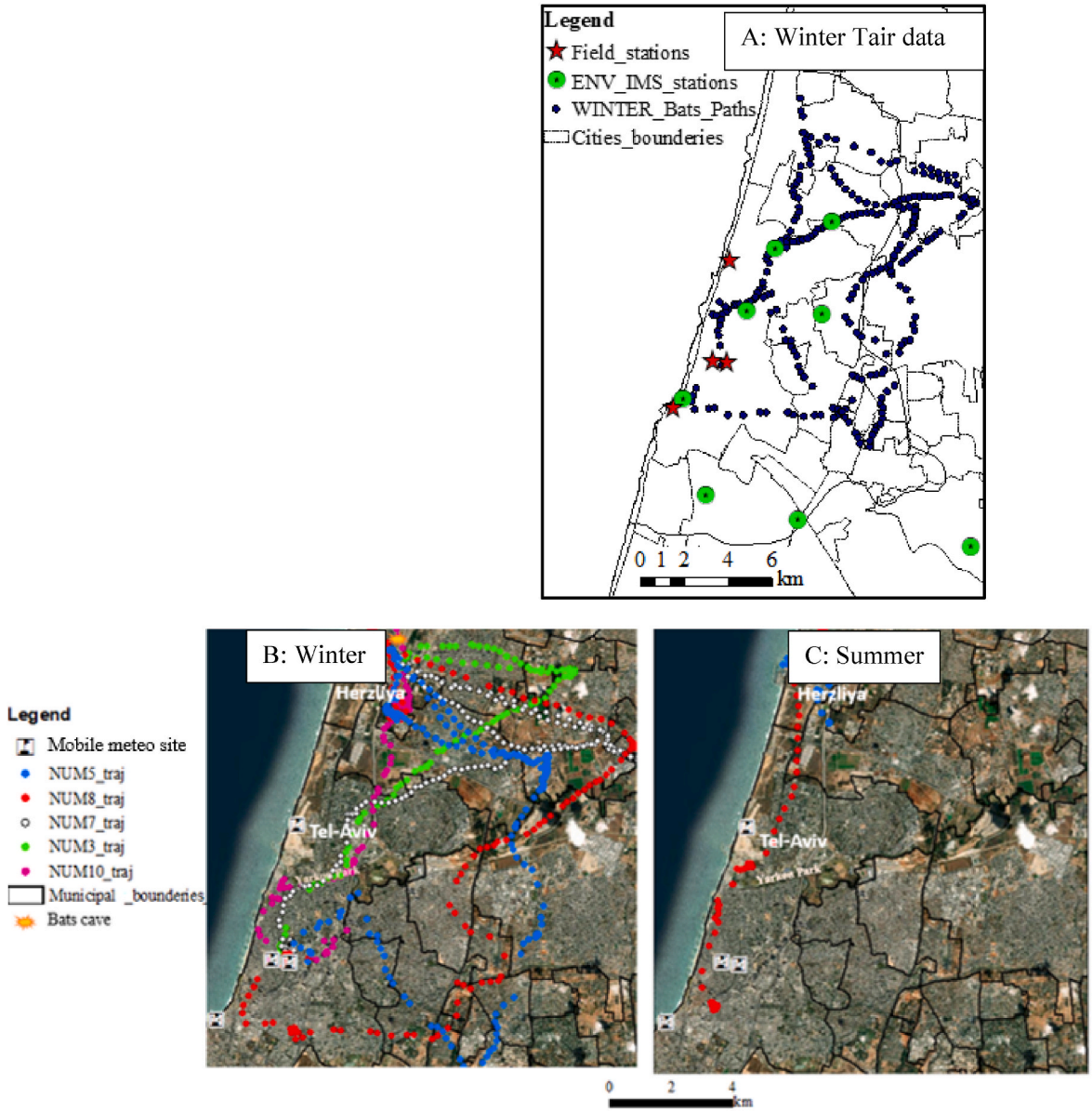

Fig. 2. Panel A: Commute flight trajectories of five bats during the winter experiment. The locations of temporal field Tair monitoring and the ground-based environmental agency monitoring sites are depicted; Panels B and C are for comparison: winter and summer commute flight trajectories (five and two bats correspondingly). The different colors represent different individual bats. Tair was measured by the bats' GPS device.

10–11 January 2019 under stable weather conditions, a clear sky and calm winds, and during the summer on 20–21 June 2019—the day of the summer solstice—under typical summer conditions with clear skies. Four mobile Campbell Scientific Inc., (USA) automatic meteorological stations were set up in the center of Tel Aviv and used to compare Tair measured by bats as well as for general spatial analyses of Tair pattern (Fig. 2). An additional station was set up in Palmachim, a rural area on the south edge of the metropolis, 1 km from the seashore. Air temperature, relative humidity, wind direction and wind velocity were measured at a standard height of 2 m, similarly to other field and Tair ground monitoring sites that aim to measure Tair at the street level (see e.g. Mandelmilch et al., 2020; Saaroni et al., 2000). Readings were taken every second and the resulting data were averaged and stored every 5 min using a Campbell Scientific data logger.

In addition, data were collected from eight official meteorological stations and similarly used as reference stations: two operated by the Israeli Meteorological Service: "Tel Aviv Coast" and "Bet Dagan" (http://www.ims.gov.il), three operated by the Israeli Ministry of Environmental Protection: "Hakfar Hayarok", "Petach Tikva" and "Holon" (http://www.svivaaqm.net). The data obtained from the meteorological stations corresponded to the duration of our experiment (20:00–02:00). Further, in Fig. 2 we show the meteorological sites that are located within the area of bats flight.

While meteorological stations continuously measure Tair at sampled location, bats related Tair readings changes in space and time. To compare between both types of measurements, we first divided our entire experiment to five different time intervals: 20–21, 21–22, 22–23,23-24, 24–02:30. The interval selection was based on the representative and statistically equal number of Tair bats-related readings for each time interval (build-in function in JMP-pro software, ver. 15). Readings of all bats were merged to generate the temporal analyses.

2.6. Modeling the impact of environmental covariates on Tair

2.6.1. Environmental covariates

The normalized difference vegetative index (NDVI) is based on red and near infrared (NIR) reflectance. In general, the NDVI is a temporal indicator of the vegetation cover and its phenological state (Lugassi et al., 2019; Tucker, 1979). It is widely used as an objective measure of the overall level of vegetation within a pixel (e.g., Sadeh et al., 2021). One Landsat 8 satellite image (level 1) from 25 December 2018, row number 38, available at a spatial resolution of 30 m × 30 m, was obtained for this study (http://earthexplorer.usgs.gov) and pre-processed. Pre-processing included radiometric conversion to radiance values for removal of atmospheric effects using a MODTRAN model (http://modtran.spectral.com/). This model estimates reflectance values for each pixel, and the latter were used as input for the NDVI calculation. We used a cloud-free satellite image overpass.

For the land cover variable, we estimated building and road percentages per 30 m × 30 m grid cell using ArcGIS software (described in Avisar et al., 2021). The building percentage was estimated using the overlay of a vector building layer (derived from aerial photographs or satellite images) on the 30 m × 30 m grid cell. Then, we summed the total built-up area per cell, and calculated the percentage coverage by the buildings out of the total cell area. We merged these values to the grid layers. For the road percentage, the following procedure was applied: The vector "roads" generally contains the total number of lanes for each road as an attribute. We used this attribute to generate a buffer around the roads. Then, the total area of the roads per cell was calculated. Finally, we also used population density within a statistical unit (MAPI: www.mapi.gov.il).

2.6.2. Modelling UHI phenomenon

The major goal of the UHI modelling using bats-based Tair readings as the major source of data (complemented by other ground-based available Tair measurements), was to study its applicability in future experimental work. To that end, first, we applied Inverse Distance Weighting (IDW) interpolation (Lyra et al., 2018). Here we compared UHI locations that were identified in the previous Saaroni et al., 2000 study that used the same technique. It was interesting to check whether we can identify areas that have undergone reconstruction, or remain the same, with a different/similar thermal pattern. Generally, the most widely used interpolation techniques (IDW, Spline, and Kriging) are governing by relatively high density of measurements and flat terrain. IDW utilize mathematical equations to create surfaces from observed points. IDW is based on the first law of geography: "everything is related to everything else, but near things are more related than distant things" (Tobler, 1970). Therefore, observations closer to an unsampled location have more influence than those at farther locations (Shepard, 1968). The method estimates values at unsampled locations according to the weighted average of the surrounding observations.

$$Zo = \sum_{i=1}^{n} Wi*Zi \quad (1)$$

where *Zo* is the estimated value, *i* and *n* are the surrounding observations, and *Wi* are the inverse distance weights. We compared our results with a previously published study (Saaroni et al., 2000) considering that areas that have undergone reconstruction may differ from the previous estimates.

Next, we used a generalized linear mixed-effects model (GLMM) to account for the effect of multiple measurements per individual. Different land-use variables within a 30 m × 30 m grid cell were examined to estimate Tair. We combined different sets of predictors, and a model was run for each set. Selection of the best model was based on the Akaike information criterion (AIC) score, a measure of the relative goodness of fit that is asymptotically related to the out-of-sample prediction R^2. Finally, the combination of predictors with the minimum AIC was selected. In adaptation to this work, the model was constructed with the following predictors: percent of the grid cell covered by buildings, roads (percentage of building surface fraction), NDVI, and time and speed of the bats' flights. Time was grouped in ~2-h intervals and the groups were examined during the total run of the experiment in winter, from 2000 h to 0230 h. The following model with random intercepts was used:

$$\text{Tair} = 1 + \text{time group} + \text{NDVI} + \text{building percentage} + \text{bat speed} + (1 / \text{bat ID}) + \text{error} \quad (2)$$

where1/bat meaning that bats' identities that were included in the model as a random factor.

Finally, Geographically weighted regression (GWR) was also estimated to investigate the spatial impact of the studied covariates on Tair. GWR was constructed in other studies and aimed to address the spatial varying effects related to the UHI phenomenon (Gao et al., 2022). GWR can be written as following (Fotheringham et al., 2002, 2003):

$$y_i = \beta_o(u_i, v_i) + \sum_{j=1}^{k} \beta_I (u_i, v_i)\, X_{ij} + \varepsilon_i \quad (3)$$

where y_i is the dependent variable; X_{ij} are the j the explanatory variables at location i. β_0 and β_j are the estimated coefficients at location i; (ui,vi) is the coordinates of location i, ε_i is the random error at location i and accounts spatial change of values. We used Ordinary Least Squares (OLS) regression to find the most explanatory variables (with the highest explained variance) (Gao et al., 2022; Wang & Chen, 2017). Based on these analyses the following variables were included in the model: NDVI, bats flight speed, time, building percentage and population density over the studied area. We tested for the multicollinearity of the studied variables (detected by a Pearson's correlation coefficient test) while excluding highly correlated variables (Gao et al., 2022).

The central part of GWR model is a weight matrix. The later represents the spatial relationship between kernel function and nearby locations (Gao et al., 2022; Yang et al., 2020). We used Gaussian functions to define the spatial weight for each statistical unit. The kernel function is a general way to construct a bandwidth. Note that larger bandwidth denotes greater effect and lower decrease of weight with distance. More detail explanation on the use of GWR model in exploring UHI spatial phenomenon can be found in Szymanowski & Kryza, 2011; Ivajnšič et al., 2014; Kim & Brown, 2021; Gao et al., 2022.

3. Results

3.1. Tair distribution: evening–early night

Fig. 2 shows the general path and flight trajectory of bats during the winter and summer experiments.

Below, we mainly refer to and analyze the differences in Tair between built-up and vegetation areas which were sampled by the bats in winter, because the summer experiment yielded too few sampling locations. Note that the summer flight trajectory was mainly along open areas which were exposed to the sea breeze in the urban part, lowering the measured Tair compared to the inner urban sites.

In Fig. 3 we show the comparison between field ground-based meteorological station Tair measurements that were deployed to validate the BAS concept. As can be seen, there is a general decrease in Tair (by 2 °C on average; maximum difference of 4–5.5 °C) from 2000 to 0230 h (upper panel, Fig. 3). These results were in good agreement with the ground-based measurements (Fig. 4, lower panel), which also verified the general decrease in Tair across different parts of the city (urban neighborhood, vegetation area, open space and airport).

3.2. Tair distribution for different land uses

To qualitatively scrutinize the data, we first presented bats' flight

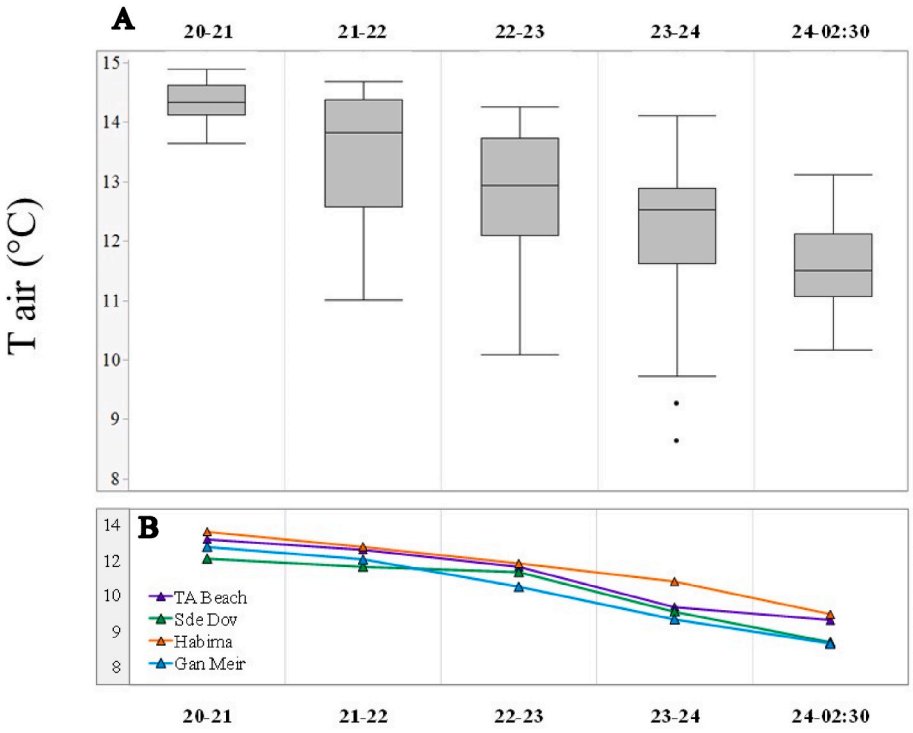

Fig. 3. A: Distribution of Tair for different time intervals as measured by the sensors on the bats. B: Tair measurements from the ground-based field experiment using mobile meteorological stations for different locations across the city (Sde-Dov, Habima, Gan-Meir). Ground-based field experiment was used for validation of the BAS experiment. Evidently similar ranges of Tair measurements were observed in each interval on-board bats and in ground-based Israeli Meteorological Service and Environmental service sites.

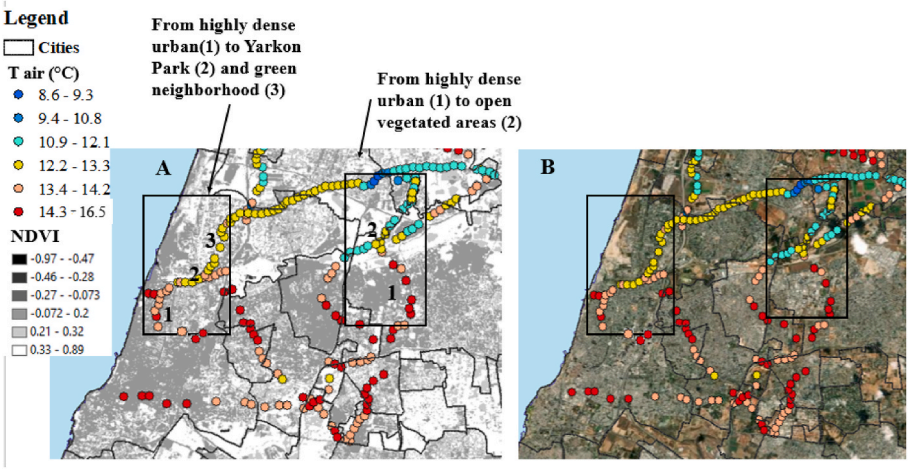

Fig. 4. Selected bats' flight paths colored according to Tair measurements. (A) NDVI image and (B) aerial photograph used as a background. Note that white and light-gray shading in panel A represent higher vegetation content whereas dark gray shading indicates lower vegetation content and more soil land coverage. Black boxes delineate two examples of changes in Tair when moving from dense urban area to vegetative area, and to open/agricultural areas.

paths on a background of NDVI values (Fig. 4A) and an aerial photograph (Fig. 4B), where each measurement is color-coded according to Tair. As can be seen, Tair clearly changed from urban areas (low NDVI) to parks and areas with high vegetation coverage (high NDVI, bright-whitish shade) but also to open agricultural parcels (low NDVI, darker gray shade). These two environmental types are highlighted by black boxes in Fig. 4.

Next, we examined the impact of vegetation on changes in Tair (Fig. 5) and found that the higher the vegetation coverage within a pixel (high NDVI value), the lower is Tair for all time intervals. Large differences in Tair between different NDVI ranges were observed between 2100 and 2200 h, with slightly smaller range between 2200 and 2400 h. The variation in Tair values within given NDVI ranges can be explained by using relatively coarse 30 m × 30 m resolution and by differences in the three-dimensional urban form. In particular, this coarse resolution limits capture of the high-resolution spatial urban heterogeneity that exists within a pixel (Sadeh et al., 2021). For example, small trees and urban spaces are only evident when using high-spatial-resolution sources. An additional source of variation is the varying soil color and its moisture levels, which might also impact the accuracy of the NDVI estimation (Huete, 1988). However, the trend of vegetation's impact on the average lowering Tair is still evident. Furthermore, below, we estimate this impact using GLMM model and show that the impact of vegetation on lowering of Tair is significant.

3.3. UHI estimation

Despite a relatively limited data set during the winter experiment, we ran IDW interpolation in the Geographic Information System (GIS) (ArcGIS Geostatistical Analyses). Fig. 6 is the iso-thermal map for the

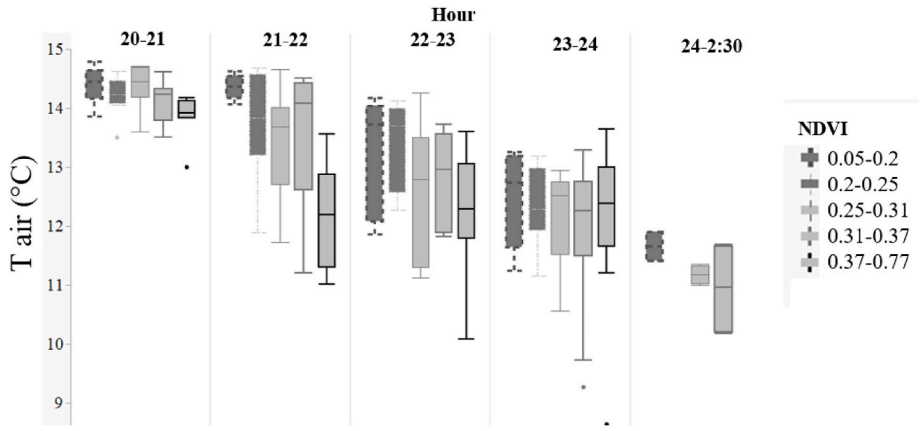

Fig. 5. Distribution of Tair for different time ranges conditioned on different NDVI values.

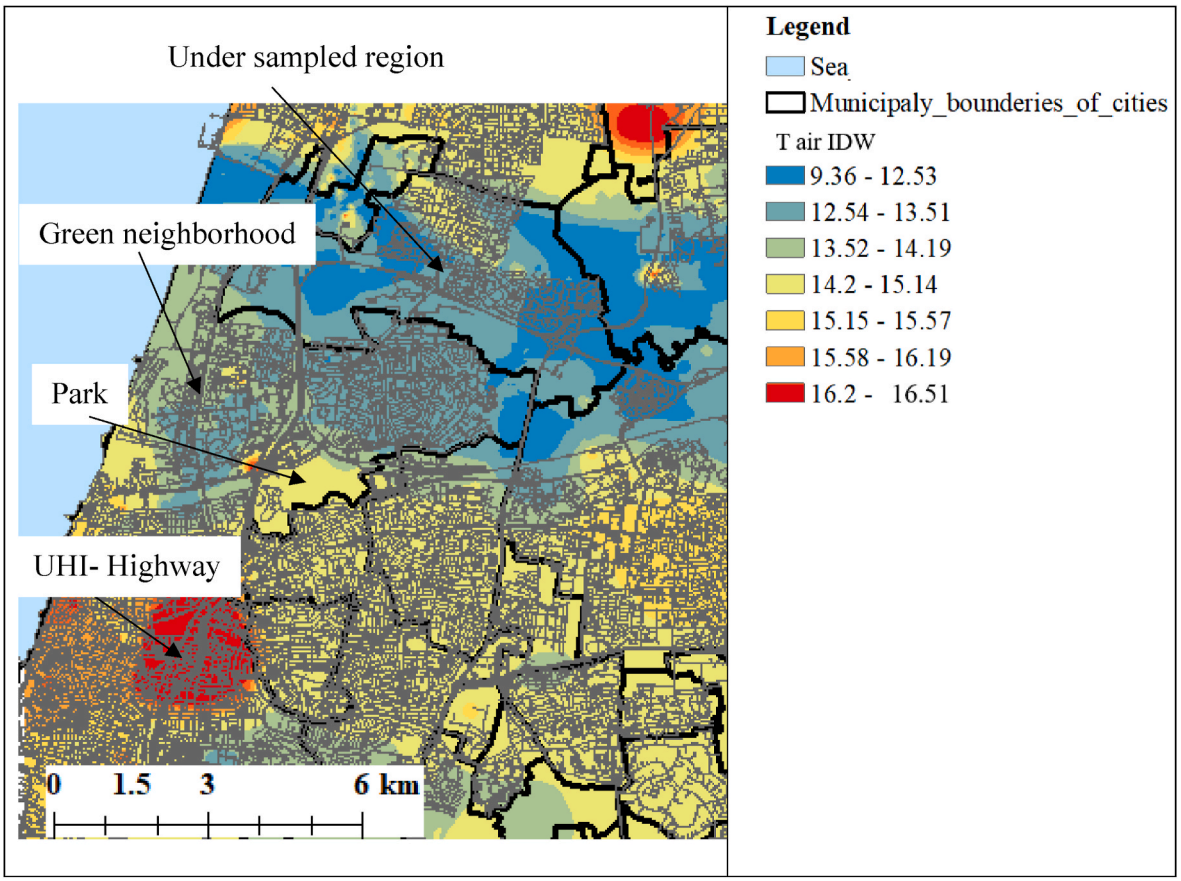

Fig. 6. IDW interpolation between different sampled locations during the winter. Overlaid on the map is a bat's trajectory color-coded according to Tair (°C). Note the Tair decrease from the dense urban area to park area, and a hot spot at the Ayalon highway intersection.

central Tel Aviv area generated based on the bats sampling. As can be seen, sampling locations where there is a lot of vegetation, as well as open vegetated spaces, were characterized by lower Tair. Importantly, we had a distinct UHI spot in the winter, centered on the Ayalon highway, at a location with numerous industrial facilities. Note that the interpolation map that we estimated using the bat-based measurements in Fig. 6 is quite comparable to previous studies that show the Ayalon highway area (highlighted as UHI in Fig. 6) as a hot spot (Pelta & Chudnovsky, 2017; Pelta et al., 2016; Saaroni et al., 2000).

3.4. Tair prediction based on a GLMM model: studying the effect of land uses

We ran a GLMM-effect with fixed effect variables in order to explain Tair: NDVI, Time, built %, flight speed and altitude (Methods). Overall the model was able to explain 65% of the variance. The fixed effects of various spatial predictors were significant proving their effect on Tair. Table 1 presents the model coefficients for all the predictors. Here, the coefficient for each key predictor shows its average effect (i.e., the common slope averaged across the groups). As evident from our results, vegetation, not surprisingly, had an average ~2 °C cooling effect. Tair also decreased by 0.5 °C from 2000 h to 0230 h. Importantly, the

Table 1
Coefficients of spatial predictors (fixed) for Tair estimation model using bat measurements (random effect coefficients were obtained for each bat used in the winter experiment).

Coefficients of spatial predictors	Estimate (°C)	*P*-value
Intercept	13.5	<0.0001
Time	−0.47	<0.0001
Bats' flight speed	0.10	<0.005
NDVI	−1.97	<0.005
Building percentage	0.01	<0.005
Flight height	0.11	0.08

Note that flight altitude was not found to be a significant variable in GLMM model. This was probably because our measurements indicated a relatively homogeneous flight height between all sampling locations with an average altitude of 3.5 m (see further analyses using GWR and Section 3.5).

average effect of flight speed on Tair was 0.1 °C. Moreover, the impact of building percentage is 0.01 °C ((over a grid cell of 30 m × 30 m).

Fig. 7 shows the results of GWR modelling. In panel A of Fig. 7 (left) we show different variables' coefficient estimates in the GWR model. For NDVI, the coefficient estimates are all negative and statistically significant ($p < 0.01$), meaning that higher green areas are associated with lower Tair. For the height of flight all estimates were negative, implying that generally, the Tair decreases with height. Similar results were found for the speed of flight (both statistically significant). The build-up percentage generally increases Tair, although its relative contribution was relatively low. Note that relative contribution of each variable differ for each spatial unit in the urban area. We might have positive (increasing) effect on some areas and negative for other locations due to differences in locations, urban characteristics, etc. Fig. 7A shows Tair estimated vs measured Tair values (right) with the overall R^2 of 0.79. The spatial estimated pattern of Tair is shown in Fig. 7 B. As can be seen, the highest Tair is along the Ayalon Highway-the busiest road of the Greater Tel-Aviv area.

3.5. UHI at three dimensions: the experimental challenge

In Fig. 8 we show Tair sampling points measured at different heights as well as sampling monitoring using bats as BAS agents. Each spatial segment location in the city was first sampled during different time intervals (Fig. 8A). Then, all intervals were combined to get a spatial view of all measurement points. Using the current set of measurements, height was not found to be a significant variable by both models that we constructed.

Although it was not possible to generate 3D UHI map on an hourly base, for some locations we were able to produce it. In Fig. 8B we show that Tair was sampled at varying heights, although most of our measurements are within 3.5 m height. In Fig. 8C we show that in a few locations we were able to measure 3D plot of Tair change (shown as points A and C, open area). Not surprisingly, the change in Tair above the dense urban area is smaller than above the vegetative area. Note also the decrease in Tair through the night. These analyses need further expansion to much larger data sets.

4. Discussion

Many animals live among us. Bats and pigeons roam the air above us while rats and other mammals dwell beneath us. With the miniaturization of suitable sensors, these animals could allow sampling environmental parameters at inaccessible locations. Animals have been used for years as biomarkers and here, we show that they can be used as sampling agents. Our manuscript thus presents a new concept of using animal-assisted sensors for urban environmental monitoring. Below, we discuss on some key findings, critically evaluating BAS approach.

4.1. Monitoring of Tair using BAS sampling vs conventional ground-based measurements

In this study, we used Egyptian fruit bats, abundant all over Israel, equipped with Vesper sensors recording location and ambient temperature logs to map the spatial Tair profile across different land uses. The selection of organism chosen for a given BAS study is subject-oriented, and in this paper, we demonstrated monitoring of the UHI phenomenon using bats. We showed the feasibility of using BAS techniques that complement existing ground-based measurements to monitor Tair in the urban environment. Importantly, we compared bats-based BAS measurements with conventional, meteorological station-based Tair measurements (Fig. 3). Our measurements and statistical analyses indicate a good agreement in Tair values for all types of measurements, indicating the feasibility and stability of light Tair sensor comparable to the conventional well-established ones.

In Table 2 we compare between bats-based BAS (as demonstrated in our paper) and conventional Tair monitoring techniques. In brief, using bats allows a faster sampling of a larger area including sampling at different heights and in locations that are inaccessible to humans (e.g., narrow passages). Bats are specifically advantageous as sensors because of their ability to cover large ranges in flight rapidly. Furthermore, the use of bats with sensors may provide a cost-effective solution for spatiotemporal measurements. In this paper, we started by comparing the bat-sourced measurements to those from a meteorological station, followed by ground-based experiments in diverse urban locations. We showed that our BAS-based measurements are largely expand Tair sampling and we were able to produce comparable to ground-based measurements results.

4.2. BAS-based method sampling limitations

The main limitation of the bat-assisted sampling method is the inability to control the bats' flight direction and height; An additional limitation was highlighted by our summer experiment where only readings from two bats were available. Specifically, in order to get the data, one needs to find the GPS after it falls off the bat. Sometimes it falls at the cave and can be found quite easily, but sometimes it falls at the foraging site and cannot be retrieved; nevertheless, its benefits are considerable, especially in areas with only a few, sparsely located ground-based monitoring stations that are costly and expensive to operate. Bats can fly at speeds of more than 50 km/h over complex terrains, and they can cover distances of hundreds of kilometers per night (Egert-Berg et al., 2018), much more than any drone; making them super agents in terms of their sampling abilities. However, the ability to get to measure Tair at different urban locations in the city that generally do not covered sufficiently by monitoring sites, using all available platforms (including BAS), is already a step forward.

It is important to mention that although scanning from the bats' routes involves an element of randomness, in this study we examined the contribution of green areas to mitigating the UHI according to the bats' flight behavior. The randomness of the sampling is quite evident, however, because the sampled locations in summer, largely consisted of open areas and areas with much lower Tair in the city (e.g., open to sea breeze effects) compared to the average measured in temporal Tair sites, we may suggest studying bats' seasonal behavior in different urban settings.

Importantly, as we already mentioned, the BAS assisted Tair sampling measurements need to be pre-processed to exclude measurements related to the bats foraging (e.g. threshold value, Section 2.5). In this regard, one need to develop algorithms that test the data representativeness and its comparativeness to the well-established ground-based data set. Application of data smoothing techniques can be also useful for less accurate Tair sensors. For much larger data sets, a "machine-learning" approach will be required for a data quality testing.

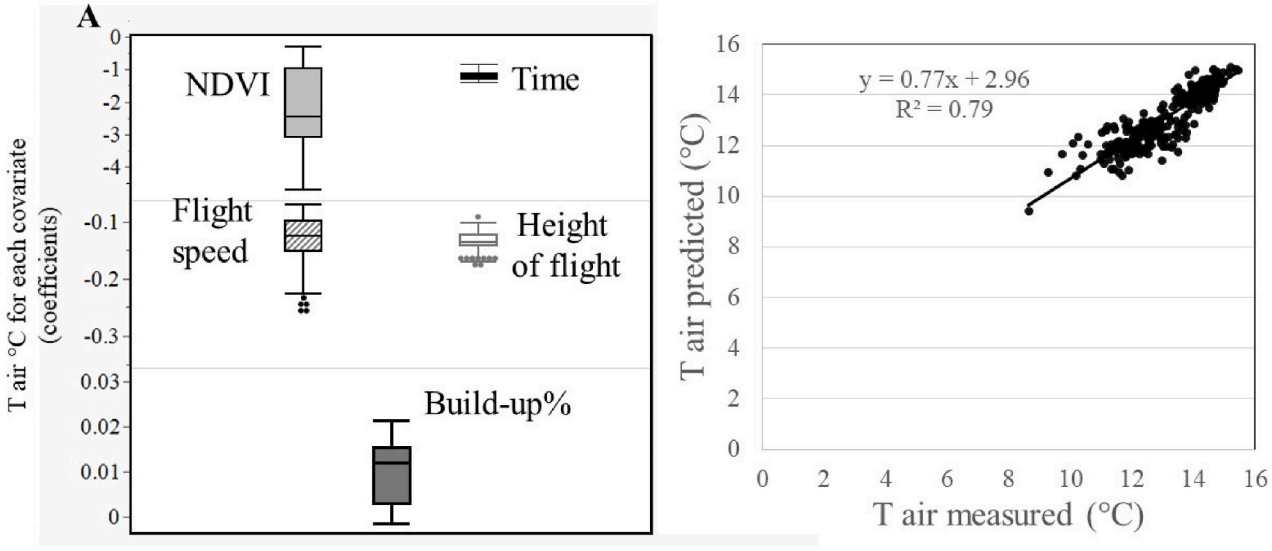

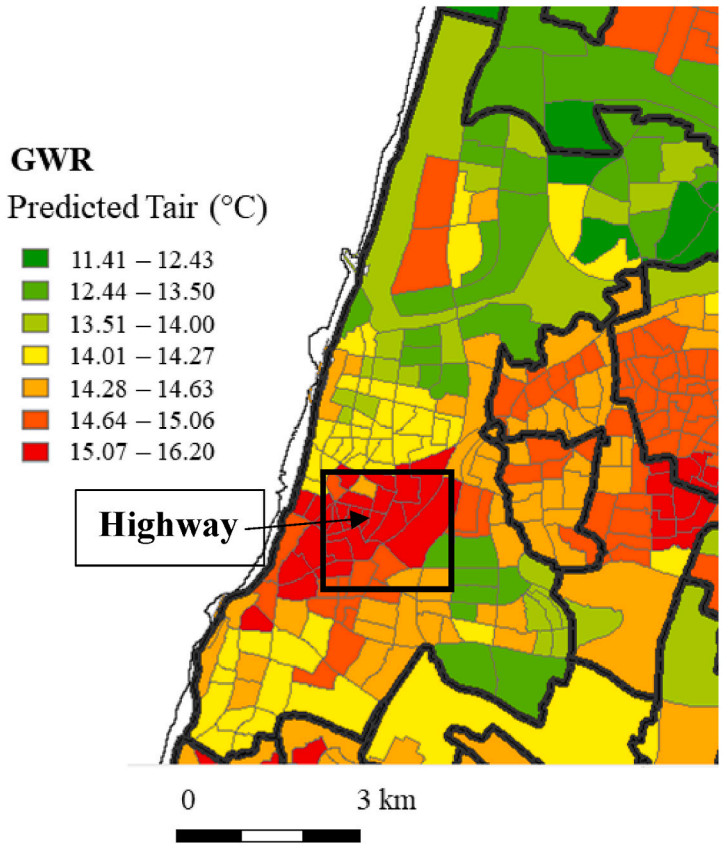

Fig. 7. The results of GWR modelling: estimated Tair using BAS and ground-based Tair monitors. Panel A: Contribution of distribution of different variables to Tair for each spatial parcel; Panel B: GWR resulted Tair estimated values.

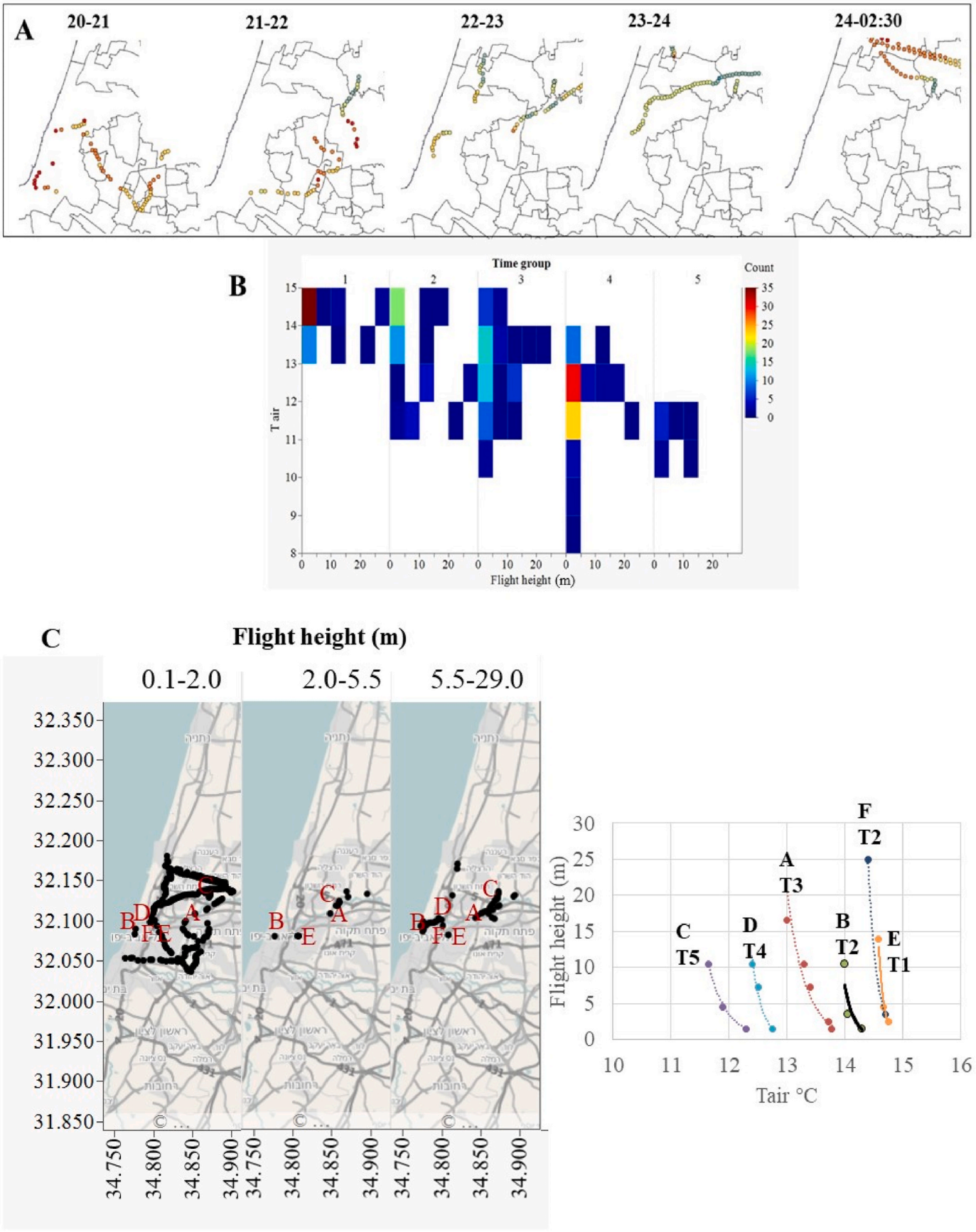

Fig. 8. Panel A: Bats spatial segment scans in the city sampled during different time; Panel B: Tair vs fight height conditioned on time (the same ranges as in Panel A). The majority of measurements are at the lower 3 m height; Panel C: Tair sampled at different heights either by bats overlap or by the same bat within 30 m distance. Right: Tair change with the height at different locations and times. T1-T5 stands for different time intervals as defined in Panel A.

Table 2
Comparison between Tair measurement platforms: BAS-based using flying organisms (bats as an example) and conventional meteorological ground-based stations.

BAS (bats)	Meteorological net-stations Monitoring methodologies
Measurement routine	
- Measures a limited range of meteorological variables, governed by the devices that can be transported by bats.the GPS is collected after it falls off the bat	- Measures a high range of meteorological variables
- Sensor can be lost if it falls at the foraging site	
- Provides dense measurements in areas with only a few, sparsely located ground-based monitoring stations, that are costly and expensive to operate	
- Devices are low-cost, available in large quantities, lightweight and mobile	- Devices are expensive. Generally, the same type of device is used at different sites based on local regulation rules of the environmental agency
- Rechargeable and operating on batteries (e.g. power source required)	- Power source required
- Spatially and vertically varies measures from "one point to another" allowing generation of 3D view map of UHI	- Measures continuously (24/7) and automatically over the same location at the same height
- Random measurements, dependent on biological variables (time of activity)	- Controlled by the user
- Relatively easy to operate	- Needs regular maintenance
Data analyses	
- Able to cover spatiotemporal phenomena in space and at different heights	- Each station covers a small and limited area at a fixed height
- Sample distribution, which is based on animals' behavior and flight paths, cannot be precisely defined in advance	
- Represents the sampled location point	- Represents the meteorological conditions of the monitoring site environment
- Data need to be pre-processed to exclude measurements from when the bats are foraging and considered for comparative representation and sampling size. For larger sample set "machine-learning" approaches would be needed for further data quality testing	- Data must be analyzed for possible outliers—"site measurement error"

4.3. UHI night-time monitoring

UHI effects are often highly localized and largely governed by local climate and proximity to the sea. It was found that at the street level, during the night in the Tel Aviv area, the UHI is more pronounced than during the daytime hours, making bats, with their nocturnal habit, ideal agents to monitor UHI effects. This result is of particular importance because not many biological species are suitable as successful BAS-based studies for UHI monitoring (Zanobetti & Schwartz, 2008; He et al., 2022). Night-time monitoring of UHI has high importance for epidemiological studies. For example, health effect studies investigating the relationship between weather and mortality, propose that a major predictor is the night-time temperature. Another study showed that night-time temperatures contribute to mortality risk in people below the age of 65 years and are crucially important to consider while developing heat–health warning systems (Murage et al., 2017). In this regard, nighttime temperature monitoring by BAS means can be further transformed to be more autonomous and robust, to map in a routine way all urban areas susceptible to the heat.

4.4. Spatial modelling and a 3D component

It is of high importance to have information on the spatial variability of UHIs across the city. This information can be used as an input in establishing of surface UHI network (Yu, Zhang, Yang, et al., 2021). Numerous studies have shown that the UHI effect varies greatly within a city, with the time of day and under different climatic conditions (Chapman et al., 2018; Cohen et al., 2012; Oke, 1987; Oliveira et al., 2011; Yu et al., 2020). Not surprisingly, our results using BAS as well as ground based Tair monitoring sites, showed a higher nighttime Tair in dense, built-up areas compared to open and highly vegetated areas (Figs. 3–5). Note that the decreasing trend of Tair with increasing vegetation appeared within every grid cell. Importantly, we have shown a larger UHI in winter than in summer, even though our summer data set was quite small. In this regard, our results agree with other studies conducted in Tel Aviv that have found UHI values at night of up to 5 °C higher temperature during the winter season compared to up to 0.8 °C temperature difference in the summer (Bitan et al., 1992; Cohen et al., 2012; Saaroni et al., 2000). Furthermore, although Tair values of urban vegetation were lower than those of built-up areas, the magnitude in Tair values varied spatially and temporally across the city and its different neighborhoods. A good example of this is the densely populated neighborhood Florentine, which showed larger Tair than any other location due to decreased air flow and convection. Another example is Tair measured in the summer along the coast, which was probably largely impacted by the sea breeze effect regardless of city location, causing a general decrease in Tair between built-up and vegetative areas. Our statistical estimation of the impact of vegetation on Tair is in good agreement with Cohen et al. (2012), who examined the diurnal and seasonal climatic behavior of green and bare urban spaces. Those authors found that in the winter, the vegetation reduces temperatures by up to 2 °C, similar to our results.

To map the UHI phenomenon, many studies apply diverse statistical models by incorporating different explanatory variables, as reviewed by Kim and Brown (Kim & Brown, 2021). Examples include linear, geographically weighted (GWR) regressions, mixed effects model, random forest, artificial neural network, deep learning (Pelta & Chudnovsky, 2017; Noi et al., 2017; Shen et al., 2022; Hrisko et al. 2020) and most recently Spatially Varying Coefficient Models with Sign Preservation (SVCM-SP) (Kim et al., 2021; Zhang et al. 2022). In the current study, several models were tested to estimate the impact of several explanatory variables on Tair. However, only during the winter experiment we have a representative data set to estimate the impact of different covariates on Tair by running the interpolation or by using mixed effects, or GWR models. In contrast, in summer, due to the small number of measurements, the model was not applicable. We showed that using both interpolation and GWR estimation, The Ayalon highway was found as a hot spot. This result is in a good agreement with previous studies conducted in our area (e.g. Pelta & Chudnovsky, 2017; Pelta et al., 2016; Saaroni et al., 2000).

Our constructed Tair model can further be enhanced to include additional covariates. Examples of such covariates include population and traffic data, atmospheric vertical parameters (boundary layer height, total water column), land cover (e.g. fractional asphalt cover, roof cover, water and soil cover), and different satellite-derived indexes (e.g. Normalized difference built-up index (NDBI)) (Oukawa et al., 2022; Zhou et al., 2020). However, a careful analysis will be required to exclude multicollinearity problem.

An additional point that needs to be generally considered in future studies is the 3D nature of the UHI phenomenon that is also governed by different urban morphology and weather conditions. This knowledge can effectively improve the interpretation of UHI as evident from recent studies (Yu, Zhang, Yang, et al., 2021; Wan-Ben et al., 2022). Using BAS method, ideally, 3D maps can be generated. Unfortunately, our study dataset did not contain enough sample points to generate such a product as most sampled points were within 3.5 m height. In spite of this limitation, we were still able to plot 3D change of Tair at several locations and these results are encouraging, showing the difference between warmer urban dense areas and cooler vegetative areas, as well as the

nocturnal temporal Tair decrease.

5. Conclusions

In this paper, we demonstrated bat bio-assisted sampling (BAS) for monitoring of the Urban Heat Island (UHI) phenomenon. We used Egyptian fruit bats equipped with low footprint sensors that record location and ambient temperature to map the Tair profiles. Our aim was to generate a better temporal and spatial understanding of the impact of different neighborhoods with different urban morphologies as a complementary data source to the existing Tair stationary network. Our results indicate the feasibility of this approach. In particular, because the differences in Tair between dense urban and open/green areas are largest during the night hours in the Mediterranean climate zone, nocturnally active bats can serve as excellent agents to monitor UHI effects.

CRediT authorship contribution statement

Chudnovsky, A-writing original draft, Writing - Review & Editing, conceptualization, investigation, methodology, formal analyses, data curation, validation, software, resources.

Goldshtein, A-formal analyses, validation, investigation, Writing - Review & Editing, conceptualization.

Shashua Bar, Limor validation, investigation, Writing - Review & Editing, conceptualization.

Yossi Yovel-methodology, investigation, validation, formal analyses, Writing - Review & Editing, conceptualization.

Oded Potchter-investigation, validation, Writing - Review & Editing, conceptualization.

Declaration of competing interest

Authors declare that they have no personal conflict of interests.

Acknowledgments

AC acknowledges Israel Science Foundation, grant no. 2461/19. The data generated in this study will be further used for air pollution studies. Authors highly appreciate proofreading and fruitful suggestions by Dr. Yoav Linzon. Authors also acknowledge Camille Vainshtein for the paper proofread. Authors highly appreciate critical comments of the annonymous reviewers.

References

Avisar, D., Pelta, R., Chudnovsky, A., & Rostkier-Edelstein, D. (2021). High resolution WRF simulations for the Tel-Aviv metropolitan area reveal the urban fingerprint in the sea-breeze hodograph. *Journal of Geophysical Research - D: Atmospheres, 126*, Article e2020JD033691. https://doi.org/10.1029/2020JD033691

Benhamou, S. (2004). How to reliably estimate the tortuosity of an animal's path: Straightness, sinuosity, or fractal dimension? *Journal of Theoretical Biology, 229*, 209–220.

Bitan, A., Noy, L., & Turk, R. (1992). The impact of the seashore on the climate of Tel-Aviv. In *Scientific reports of the Institute for meteorology and climate research of karlsruhe university* (Vol. 16, pp. 147–160). Karlsruhe, Germany: KIT Scientific Publishing.

Bitan, A., & Rubin, S. (1994). *Climatic atlas of Israel for physical and EnvPlanning and design*. Tel-Aviv: Ramot Publishing Co.

Brauer, M., & Hystad, P. (2014). Commentary: Cities and health…Let me count the ways. *Epidemiology, 25*(4), 526–527.

Burgués, J., & Marco, S. (2020). Environmental chemical sensing using small drones: A review. *The Science of the Total Environment, 748*, Article 141172. https://doi.org/10.1016/j.scitotenv.2020.141172

Carreras, H. A., & Pignata, M. L. (2002). Biomonitoring of heavy metals and air quality in Cordoba City, Argentina, using transplanted lichens. *Environmental Pollution, 117*(1), 77–87.

Carreras, H. A., Wannaz, E. D., Perez, C. A., & Pignata, M. L. (2005). The role of urban air pollutants on the performance of heavy metal accumulation in *Usnea amblyoclada*. *Environmental Research, 97*(1), 50–57.

Carreras, H. A., Wannaz, E. D., & Pignata, M. L. (2009). Pignata, Assessment of human health risk related to metals by the use of biomonitors in the province of Córdoba, Argentina. *Environmental Pollution, 157*(1), 117–122.

Carreras, H., Zanobetti, A., & Koutrakis, P. (2015). Effect of daily temperature range on respiratory health in Argentina and its modification by impaired socio-economic conditions and PM10 exposures. *Environmental Pollution, 206*, 175–182. https://doi.org/10.1016/j.envpol.2015.06.037

Chapman, S., Thatcher, M., Salazar, A., Watson, J. E. M., & McAlpine, C. A. (2018). The effect of urban density and vegetation cover on the heat island of a subtropical city. *Journal of Applied Meteorology and Climatology, 57*(11), 2531–2550.

Charrassin, J.-B., Park, Y.-H., Maho, Y. L., & Bost, C.-A. (2002). Penguins as oceanographers unravel hidden mechanisms of marine productivity. *Ecology Letters, 5*, 317–319. https://doi.org/10.1046/j.1461-0248.2002.00341.x

Chudnovsky, A., Ben-Dor, E., & Saaroni, H. (2004). Diurnal thermal behavior of selected urban objects using remote sensing measurements. *Energy and Buildings, 36*(11), 1063–1074.

Cohen, P., Potchter, O., & Matzarakis, A. (2012). Daily and seasonal climatic conditions of green urban open spaces in the mediterranean climate and their impact on human comfort. *Building and Environment, 51*(May), 285–295.

Costa, D. P., Huckstadt, L. A., Crocker, D. E., McDonald, B. I., Goebel, M. E., & Fedak, M. A. (2010). Approaches to studying climatic change and its role on the habitat selection of Antarctic pinnipeds. *Integrative and Comparative Biology, 50*, 1018–1030.

Cvikel, N., et al. (2015). On-board recordings reveal no jamming avoidance in wild bats. *Proceedings of the Royal Society B: Biological Sciences, 282*.

Cvikel, D., Kahanov, Y., Rosen, B., Saaroni, H., & Galili, E. (2014). The voyage of leucippe and clitophon: A new interpretation. *Mariners Mirror, 100*(4), 388–404. https://doi.org/10.1080/00253359.2014.962265

Daniel, S., Korine, C., & Pinshow, B. (2008). Central-place foraging in nursing, arthropodgleaning bats. *Canadian Journal of Zoology, 86*(7), 623–626. https://doi.org/10.1139/Z08-041

Deilami, K., Kamruzzaman, M., & Liu, Y. (2018). Urban heat island effect: A systematic review of spatio-temporal factors, data, methods, and mitigation measures. *International Journal of Applied Earth Observation and Geoinformation, 67*, 30–42.

Egert-Berg, K., Hurme, E. R., Greif, S., Goldstein, A., Harten, L., Herrera, M. L. G., & Yovel, Y. (2018). Resource ephemerality drives social foraging in bats. *Current Biology, 28*, 1–7.

Fotheringham, A. S., Brunsdon, C., & Charlton, M. (2002). *Geographically weighted regression:the analysis of spatially varying relationships. Chichester: Wiley (6) (PDF) Geographically Weighted Regression: The Analysis of Spatially Varying Relationships*. Available from: https://www.researchgate.net/publication/27246972_Geographically_Weighted_Regression_The_Analysis_of_Spatially_Varying_Relationships. (Accessed 31 March 2023).

Fotheringham, A. S., Brunsdon, C., & Charlton, M. (2003). *Geographically weighted regression: the analysis of spatially varying relationships*. West Sussex, England: John Wiley & Sons.

Gao, Y., Zhao, J., & Han, L. (2022). Exploring the spatial heterogeneity of urban heat island effect and its relationship to block morphology with the geographically weighted regression model. *Sustainable Cities and Society, 76*, Article 103431. https://doi.org/10.1016/j.scs.2021.103431. ISSN 2210-6707.

Goldshtein, A., Harten, L., & Yovel, Y. (2021). Mother bats facilitate pup navigation learning. *Current Biology, 32*(2), 350–360. https://doi.org/10.1016/j.cub.2021.11.010

Greif, S., & Yovel, Y. (2019). Using on-board sound recordings to infer behaviour of free-moving wild animals. *Journal of Experimental Biology, 222*.

Hankey, S., & Marshall, J. D. (2017). Urban Form, Air pollution, and health. *Current Environmental Health Reports, 4*(4), 491–503. https://doi.org/10.1007/s40572-017-0167-7

Harten, L., Katz, A., Goldshtein, A., Handel, M., & Yovel, Y. (2020). The ontogeny of a mammalian cognitive map in the real world. *Science, 369*(6500), 194–197. https://doi.org/10.1126/science.aay3354. PMID: 32647001.

Hays, S. M., Becker, R. A., Leung, H. W., Aylward, L. L., & Pyatt, D. W. (2007). Biomonitoring equivalents: A screening approach for interpreting biomonitoring results from a public health risk perspective. *Regulatory Toxicology and Pharmacology, 47*(1), 96–109. https://doi.org/10.1016/j.yrtph.2006.08.004. ISSN 0273-2300.

He, C., Kim, H., Hashizume, M., Lee, W., Honda, Y., Kim, S. E., Kinney, P. L., Schneider, A., Zhang, Y., Zhu, Y., Zhou, L., Chen, R., & Kan, H. (2022). The effects of night-time warming on mortality burden under future climate change scenarios: A modelling study. *The Lancet Planetary Health, 6*(8), e648–e657. https://doi.org/10.1016/S2542-5196(22)00139-5. PMID: 35932785.

Holt, E. A., & Miller, S. W. (2010). Bioindicators: Using organisms to measure environmental impacts. *Natural Educational Knowledge, 3*(10), 8.

Hrisko, J., Ramamurthy, P., Yu, Y., Yu, P., & Melecio-Vázquez, D. (2020). Urban air temperature model using GOES-16 LST and a diurnal regressive neural network algorithm. *Remote Sensing of Environment, 237*, Article 111495. https://doi.org/10.1016/j.rse.2019.111495

Huete, A. R. (1988). A soil-adjusted vegetation index (SAVI). *Remote Sensing of Environment, 25*, 295–309. https://doi.org/10.1016/0034-4257(88)90106-X

Ivajnšič, D., Kaligarič, M., & Žiberna, I. (2014). Geographically weighted regression of the urban heat island of a small city. *Applied Geography, 53*, 341–353.

Kezoudi, M., Keleshis, C., Antoniou, P., Biskos, G., Bronz, M., Constantinides, C., Desservettaz, M., Gao, R., Girdwood, J., Harnetiaux, J., Kandler, K., Leonidou, A., Liu, Y., Lelieveld, J., Marenco, F., Mihalopoulos, N., Močnik, G., Neitola, K., Paris, J., … Sciare, J. (2021). The unmanned systems research laboratory (USRL): A new facility for UAV-based atmospheric observations. *Atmosphere, 12*(8), 1042. https://doi.org/10.3390/atmos12081042. https://www.mdpi.com/2073-4433/12/8/1042

Kim, M., Wang, L., & Zhou, Y. (2021). Spatially varying coefficient models with sign preservation of the coefficient functions. *JABES, 26*, 367–386. https://doi.org/10.1007/s13253-021-00443-5

Kim, S. W., & Brown, R. D. (2021). Urban heat island (UHI) intensity and magnitude estimations: A systematic literature review. *The Science of the Total Environment, 779*, Article 146389.

Köppen, W. P. (1931). *Grundriss der klimakunde*. Berlin: W. de Gruyter.

Kuantama, E., Tarca, R., Dzitac, S., Dzitac, I., Vesselenyi, T., & Tarca, I. (2019). The design and experimental development of air scanning using a sniffer quadcopter. *Sensors, 19*(18), 3849. https://doi.org/10.3390/s19183849

Lavi, A., Potchter, O., Omer, I., & Fireman, E. (2016). Mapping air pollution by biological monitoring in the metropolitan Tel Aviv area. *International Journal of Environmental Health Research, 26*(3), 346–360.

Lensky, I. M., & Dayan, U. (2015). Satellite observations of land surface temperature patterns induced by synoptic circulation. *International Journal of Climatology, 35*, 189–195. https://doi.org/10.1002/joc.3971

Luber, G., & McGeehin, M. (2008). Climate change and extreme heat events. *American Journal of Preventive Medicine, 35*(5), 429–435.

Lugassi, R., Blank, A., Rogozovsky, I., Ohneiser, K., Ansmann, A., Linzon, Y., & Chudnovsky, A. (2022). *From laboratory to in-situ 3D measurements of complex pollution states in the city: Introducing a general concept using compact multisensory assemblies on UAVs*. Atmospheric Environment. Accepted (April 30,.

Lugassi, R., Zaady, E., Goldshleger, N., Shoshany, M., & Chudnovsky, A. (2019). Spatial and temporal monitoring of pasture ecological quality: Sentinel-2-based estimation of crude protein and neutral detergent fiber contents. *Remote Sensing, 11*, 799.

Lyra, G. B., Correia, T. P., de Oliveira-Junior, J. F., & Zeri, M. (2018). Evaluation of methods of spatial interpolation for monthly rainfall data over the state of Rio de Janeiro, Brazil. *Theoretical and Applied Climatology, 134*, 955–965.

Mandelmilch, M., Ferenz, M., Mandelmilch, N., & Potchter, O. (2020). Urban spatial patterns and heat exposure in the Mediterranean city of Tel Aviv. *Atmosphere, 11*, 963. https://doi.org/10.3390/atmos11090963

Murage, P., Hajat, S., & Kovats, R. S. (2017). Effect of night-time temperatures on cause and age-specific mortality in London. *Environmental Epidemiology, 1*(2), Article e005. https://doi.org/10.1097/EE9.0000000000000005. Epub 2017 Dec 13. PMID: 33195962; PMCID: PMC7608908.

Noi, P. T., Degener, J., & Kappas, M. (2017). Comparison of multiple linear regression, cubist regression, and random forest algorithms to estimate daily air surface temperature from dynamic combinations of MODIS LST data. *Remote Sensing, 9*. https://doi.org/10.3390/rs9050398

Oke, T. R. (1987). *Boundary layer climates*. Oxfordshire, UK: Routledge.

Olsson, O., & Brown, J. S. (2006). The foraging benefits of information and the penalty of ignorance. *Oikos, 112*, 260–273. https://doi.org/10.1111/j.0030-1299.2006.13548.x

Oliveira, S., Andrade, H., & Vaz, T. (2011). The cooling effect of green spaces as a contribution to the mitigation of urban heat: A case study in lisbon. *Building and Environment, 46*(11), 2186–2194.

Oukawa, G. Y., Krecl, P., & Targino, A. C. (2022). Fine-scale modeling of the urban heat island: A comparison of multiple linear regression and random forest approaches. *Science of the Total Environment, 815*, Article 152836.

Pelta, R., & Chudnovsky, A. A. (2017). Spatiotemporal estimation of air temperature patterns at the street level using high resolution satellite imagery. *The Science of the Total Environment, 579*, 675–684.

Pelta, R., Chudnovsky, A. A., & Schwartz, J. (2016). Spatio-temporal behavior of brightness temperature in Tel-Aviv and its application to air temperature monitoring. *Environmental Pollution, 208*(A), 153–160.

Pollack, L., Ondrasek, N. R., & Calisi, R. (2017). Urban health and ecology: The promise of an avian biomonitoring tool. *Current Zoology, 63*(2), 205–212. https://doi.org/10.1093/cz/zox011

Potchter, O., & Saaroni, H. (1998). An examination of the map of climatic regions of Israel, according to the Koppen classification. *Studies in the Geography of Israel, 15*, 179–194 (in Hebrew).

Rotem-Mindali, O., Michael, Y., Helman, D., & Lensky, I. M. (2015). The role of local land-use on the urban heat island effect of Tel Aviv as assessed from satellite remote sensing. *Applied Geography, 56*(2015), 145–153.

Saaroni, H., Ben-Dor, E., Bitan, A., & Potchter, O. (2000). Spatial distribution and micro-scale characteristics of the urban heat island in Tel-Aviv, Israel. *Landscape and Urban Planning, 48*, 1–18.

Sadeh, M., Brauer, M., Dankner, R., Fulman, N., & Chudnovsky, A. (2021). Remote sensing metrics to assess exposure to residential greenness in epidemiological studies: A population case study from the eastern mediterranean. *Environment International, 146*, Article 106270.

Salvador, C., Gullón, P., Franco, M., & Vicedo-Cabrera, A. W. (2023). Heat-related first cardiovascular event incidence in the city of Madrid (Spain): Vulnerability assessment by demographic, socioeconomic, and health indicators. *Environmental Research.* , Article 115698. https://doi.org/10.1016/j.envres.2023.115698

Santonen, T., Aitio, A., Fowler, B. A., & Nordberg, M. (2015). Chapter 8 - biological monitoring and biomarkers. In G. F. Nordberg, & B. A. Fowler (Eds.), *Monica nordberg, handbook on the toxicology of metals* (4th ed.). Academic Press, 2015, 155-171, ISBN 978044459453.

Shashua-Bar, L., & Hoffman, M. E. (2000). Vegetation as a climatic component in the design of an urban street: An empirical model for predicting the cooling effect of urban green areas with trees. *Energy and Buildings, 31*(3), 221–235.

Shashua-Bar, L., Potchter, O., Bitan, A., Boltansky, D., & Yaakov, Y. (2010). Microclimate modelling of street tree species effects within the varied urban morphology in the Mediterranean city of Tel Aviv. *Israel International Journal of Climatology, 30*(1), 44–57.

Shen, C., Hou, H., Zheng, Y., Murayama, Y., Wang, R., & Hu, T. (2022). Prediction of the future urban heat island intensity and distribution based on landscape composition and configuration: A case study in Hangzhou. *Sustainable Cities and Society, 83*, Article 103992. https://doi.org/10.1016/j.scs.2022.103992

Shepard, D. (1968). A two-dimensional interpolation function for irregularly-spaced data. In *Acm '68: Proceedings of the 1968 23rd ACM national conference* (pp. 517–524). https://doi.org/10.1145/800186.810616

Smargiassi, A., Goldberg, M. S., Plante, C., Fournier, M., Baudouin, Y., & Kosatsky, T. (2009). Variation of daily warm season mortality as a function of micro-urban heat islands. *Journal of Epidemiology & Community Health, 63*(8), 659–664. https://doi.org/10.1136/jech.2008.078147

Szymanowski, M., & Kryza, M. (2011). Application of geographically weighted regression for modelling the spatial structure of urban heat island in the city of Wroclaw (SW Poland). *Procedia Environmental Sciences, 3*. https://doi.org/10.1016/j.proenv.2011.02.016, 1878-0296.

Tobler, W. (1970). A computer movie simulating urban growth in the Detroit region. *Economic Geography, 46*, 234–240.

Tsoar, A., Nathan, R., Bartan, Y., Vyssotski, A., Dell'Omo, G., & Ulanovsky, N. (2011). Large-scale navigational map in a mammal. *Proceedings of the National Academy of Sciences of the United States of America, 108*, E718–E724.

Tucker, C. J. (1979). Red and photographic infrared linear combinations for monitoring vegetation. *Remote Sensing of Environment, 8*(2), 127–150. ISSN 0034-4257.

Ulpiani, G. (2021). On the linkage between urban heat island and urban pollution island: Three-decade literature review towards a conceptual framework. *The Science of the Total Environment, 751*, Article 141727. https://doi.org/10.1016/j.scitotenv.2020.141727

Walendziuk, W., Szatylowicz, E., Oldziej, D., & Slowik, M. (2018). Unmanned aerial vehicle as a measurement tool in engineering and environmental protection. In *Proceedings volume 10808, photonics applications in astronomy, communications, industry, and high-energy physics experiments* (pp. 1749–1757). https://doi.org/10.1117/12.2501378, 2018.

Wan-Ben, W., Zhao-Wu, Y., Ma, J., & Zhao, B. (2022). Quantifying the influence of 2D and 3D urban morphology on the thermal environment across climatic zones. *Landscape and Urban Planning, 226*, Article 104499.

Wang, C.-H., & Chen, N. (2017). A geographically weighted regression approach to investigating the spatially varied built-environment effects on community opportunity. *Journal of Transport Geography, 62*, 136–147. ISSN 0966-6923.

Wang, Y., Guo, Z., & Han, J. (2021). The relationship between urban heat island and air pollutants and them with influencing factors in the Yangtze River Delta, China. *Ecological Indicators, 129*, Article 107976.

Wilmers, C. C., Nickel, B., Bryce, C. M., Smith, J. A., Wheat, R. E., & Yovovich, V. (2015). The golden age of bio-logging: How animal-borne sensors are advancing the frontiers of ecology. *Ecology, 96*, 1741–1753. https://doi.org/10.1890/14-1401.1

WMO. (2018). *Guide to climatological practices*. Geneva, Switzerland: WMO.

Yang, Q., Yuan, Q., Yue, L., & Li, T. (2020). Investigation of the spatially varying relationships of PM2.5 with meteorology, topography, and emissions over China in 2015 by using modified geographically weighted regression. *Environmental Pollution, 262*(4), Article 114257. https://doi.org/10.1016/j.envpol.2020.114257, 2020.

Yu, Z., Yang, G., Zuo, S., Jørgensen, G., Koga, M., & Vejre, H. (2020). Critical review on the cooling effect of urban blue-green space: A threshold-size perspective. *Urban Forestry and Urban Greening, 49*, Article 126630. https://doi.org/10.1016/j.ufug.2020.126630

Yu, Z., Zhang, J., Yang, G., & Schlaberg, J. (2021). Reverse thinking: A new method from the graph perspective for evaluating and mitigating regional surface heat islands. *Remote Sensing, 13*, 1127. https://doi.org/10.3390/rs13061127

Zanobetti, A., & Schwartz, J. (2008). Temperature and mortality in nine US cities. *Epidemiology, 19*, 563.

Zhang, T., Zhou, Y., Wang, L., Zhao, K., & Zhu, Z. (2022). Estimating 1 km gridded daily air temperature using a spatially varying coefficient model with sign preservation. *Remote Sensing of Environment, 277*, Article 113072. https://doi.org/10.1016/j.rse.2022.113072P.T

Zhou, B., Erell, E., Hough, I., Rosenblatt, J., Just, A. C., Novack, V., & Kloog, I. (2020). Estimating near-surface air temperature across Israel using a machine learning based hybrid approach. *International Journal of Climatology, 40*, 6106–6121. https://doi.org/10.1002/joc.6570